Photoinduced PCET in Ruthenium – Phenol Systems: Thermodynamic Equivalence of Uni- and Bidirectional Reactions

Journal:	*Inorganic Chemistry*
Manuscript ID:	ic-2015-00318g
Manuscript Type:	Article
Date Submitted by the Author:	10-Feb-2015
Complete List of Authors:	Nomrowski, Julia; University of Basel, Department of Chemistry Wenger, Oliver; University of Basel, Department of Chemistry

Photoinduced PCET in Ruthenium – Phenol Systems: Thermodynamic Equivalence of Uni- and Bidirectional Reactions

*Julia Nomrowski, and Oliver S. Wenger**

Department of Chemistry, University of Basel, St. Johanns-Ring 19, CH-4056 Basel, Switzerland

ABSTRACT

Six termolecular reaction systems comprised of Ru(4,4'-bis(trifluoromethyl)-2,2'-bipyridine)$_3^{2+}$, phenols with different *para*-substituents, and pyridine in acetonitrile undergo proton-coupled electron transfer (PCET) upon photoexcitation of the metal complex. Five of these six phenols are found to release in concerted fashion an electron to the ruthenium photooxidant and a proton to the pyridine base. The kinetics for this concerted bidirectional PCET process and its relationship to the reaction free energy were compared to the driving-force dependence of reaction kinetics for unidirectional concerted proton-electron transfer (CPET) between the same phenols and Ru(2,2'-bipyrazine)$_3^{2+}$, a combined electron/proton acceptor. The results strongly support the concept of thermodynamic equivalence between separated electron/proton acceptors

and single-reagent hydrogen-atom acceptors. A key feature of the explored systems is the similarity between molecules employed for bi- and unidirectional CPET.

INTRODUCTION

Proton-coupled electron transfer (PCET) can occur either in consecutive electron transfer (ET) and proton transfer (PT) steps (in whatever sequence) or in concerted fashion, i. e., via a so-called concerted proton-electron transfer (CPET) mechanism.[1] A hallmark of the CPET mechanism is the avoidance of charged reaction intermediates, and therefore this process is often associated with significantly lower activation barriers than consecutive ET-PT or PT-ET mechanisms.[2]

So-called unidirectional PCET resembles hydrogen-atom transfer (HAT) in that the direction of electron and proton transfer is the same, i. e., a combined electron/proton donor reacts with a combined electron/proton acceptor. In bidirectional PCET, also called multi-site electron-proton transfer, more than two reaction partners are involved. A typical scenario is that a combined electron/proton donor releases its electron to an oxidant while its proton is transferred to a (separate) base. Phenols are a frequent choice as combined electron/proton donors because the phenolic proton becomes acidic upon oxidation.[3] Neutral phenols are not acidic in the solvents typically used for such studies, and consequently PT-ET mechanisms are less important. Moreover, O-H donors react at inherently faster rate that C-H donors.[4]

In recent years, there have been numerous mechanistic studies of uni- and bidirectional CPET,[5] and it has become clear that similar thermochemical considerations are useful for both reaction types.[6] However, the sets of reactants which are employed for experimental studies of

unidirectional CPET are often very different from those used for investigations of bidirectional CPET. Here, we report results which permit a direct comparison of uni- and bidirectional CPET because the employed reactants are very similar in both reaction types.

In a prior study we have found that unidirectional PCET between 6 different phenols and photoexcited $Ru(bpz)_3^{2+}$ (bpz = 2,2'-bipyrazine) occurs predominantly via a CPET mechanism (Scheme 1a).[7] Here, we report on bidirectional CPET involving the same phenols as combined electron/proton donors, photoexcited $Ru((CF_3)_2bpy)_3^{2+}$ ($(CF_3)_2bpy$ = 4,4'-bis(trifluoromethyl)-2,2'-bipyridine) as an electron acceptor, and pyridine as a base (Scheme 1b). Change of the *para*-substituents of the phenols (R-PhOH) along the series R = OCH_3, CH_3, H, Cl, Br, CN permits systematic variation of the O-H bond dissociation free energy (BDFE) from 83.0 to 92.6 kcal/mol.[3, 8]

Scheme 1. (a) Unidirectional CPET between phenols and photoexcited Ru(2,2'-bipyrazine)$_3^{2+}$ as investigated previously;[7a] (b) bidirectional CPET between photoexcited $Ru((CF_3)_2bpy)_3^{2+}$, phenols, and pyridine as investigated in this work. ET = electron transfer, PT = proton transfer. R = OCH_3, CH_3, H, Cl, Br, CN.

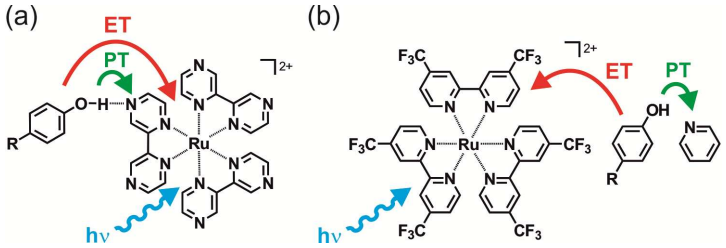

RESULTS AND DISCUSSION

Simple electron transfer. Photoexcited $Ru((CF_3)_2bpy)_3^{2+}$ in CH_3CN is a rather strong oxidant with a reduction potential of 0.9 V vs. Fc^+/Fc in its relatively long-lived ^{3}MLCT excited state.[9] However, in CH_3CN the 6 phenols from Scheme 1 are all oxidized at even more positive potentials (Table 1).[10]

Table 1. Electrochemical potentials (in V vs. Fc^+/Fc) for one-electron oxidation of the individual phenols in CH_3CN, pK_a values of the neutral phenols in CH_3CN, pK_a values of the respective phenoxyl radical cations in CH_3CN, experimental O-H bond dissociation free energies (BDFEs; in kcal/mol) in dimethylsulfoxide, and estimated BDFEs in CH_3CN.

R	E(R-PhOH$^{+/0}$)[a]	pK_a (R-PhOH)	pK_a (R-PhOH$^+$)[b]	$BDFE_{DMSO}$[d]	$BDFE_{MeCN}$[e]
CH_3O	1.05	31.0[b]	6.8	83.0	82.8
CH_3	1.16	27.5[c]	8.4	87.1	86.3
H	1.25	26.6[c]	4.8	88.3	88.3
Cl	1.25	25.4[c]	1.5	88.7	88.3
Br	1.23	25.5[c]	3.8	89.1	89.1
CN	1.40	22.7[c]	-0.4	92.6	92.7

[a] From ref. [10]. [b] Calculated on the basis of pK_a values for DMSO reported in refs. [3, 8] using the procedure described in ref. [11]. [c] From ref. [12]. [d] From refs. [3, 8]. [e] Calculated for CH_3CN solution from gas phase bond dissociation enthalpies as described in the text (see Supporting Information for details);[8, 13] error bars are on the order of ±1.5 kcal/mol.

Consequently, 5 out of the 6 considered phenols are unable to quench the ^{3}MLCT luminescence emitted by $Ru((CF_3)_2bpy)_3^{2+}$ in pure CH_3CN. Only 4-methoxyphenol (CH_3O-PhOH) is a sufficiently strong electron donor to induce some detectable luminescence quenching by photoinduced electron transfer (Figure S1). Stern-Volmer analysis of steady-state and time-resolved luminescence data (Figure S2) leads to the conclusion that the rate constant for

bimolecular electron transfer from CH_3O-PhOH to photoexcited $Ru((CF_3)_2bpy)_3^{2+}$ is k_{ET} = $(7.0\pm0.4)\cdot10^7$ M^{-1} s^{-1} in CH_3CN at 20 °C. As far as the 5 other phenols are concerned, given a ^{3}MLCT lifetime of ~580 ns for $Ru((CF_3)_2bpy)_3^{2+}$ in aerated CH_3CN and the lack of any detectable luminescence quenching for phenol concentrations of up to 0.55 M (in absence of any base), one can conclude that the upper limit of k_{ET} for the phenols with R = CH_3, H, Cl, Br, CN is 10^5 M^{-1} s^{-1}. In other words, simple (i. e., not proton-coupled) electron transfer is inefficient for all phenols except 4-methoxyphenol. For the latter it is moderately efficient.

Photochemistry in presence of pyridine. When pyridine is present in CH_3CN, phenol concentrations on the order of 0.3 M lead to readily detectable ^{3}MLCT luminescence quenching in all 6 cases. This is exemplified by the luminescence data obtained with CH_3-PhOH shown in Figure 1. Analogous data for the 5 other phenol / ruthenium reaction couples can be found in the Supporting Information (Figures S3 – S7). Figure 1a shows steady-state luminescence spectra obtained from aerated CH_3CN solutions containing $Ru((CF_3)_2bpy)_3^{2+}$ ($2\cdot10^{-5}$ M) in presence of a fixed concentration of CH_3-PhOH (42 mM) but variable pyridine concentrations (see inset). Excitation occurred at 450 nm, i. e., selectively into the ^{1}MLCT absorption band of $Ru((CF_3)_2bpy)_3^{2+}$. As the pyridine concentration increases from 0 to 1.23 M, the $Ru((CF_3)_2bpy)_3^{2+}$ ^{3}MLCT luminescence intensity decreases by roughly 20%. The ^{3}MLCT luminescence lifetime (measured after pulsed excitation at 532 nm) decreases from 580 ns in pure aerated CH_3CN to 460 ns in presence of 1.23 M pyridine, i. e., the lifetime shortens by 21%. In a control experiment with $2\cdot10^{-5}$ M $Ru((CF_3)_2bpy)_3^{2+}$ in CH_3CN and pyridine concentrations varying between 0 and 1.0 M but containing no phenol, the luminescence intensity does not decrease and the luminescence lifetimes are unchanged (Figure S8). Thus it is clear that CH_3-PhOH and pyridine must be simultaneously present in order to quench the emission. The same is

true for the phenols with R = H, Cl, Br, CN. For 4-methoxyphenol (R = OCH_3) there is some emission quenching already in absence of pyridine as discussed above (Figures S1, S2), but pyridine addition at constant CH_3O-PhOH concentration makes emission quenching markedly more efficient (Figure S3). Thus, for all 6 phenols the presence of pyridine is crucial for inducing substantial $Ru((CF_3)_2bpy)_3^{2+}$ luminescence quenching.

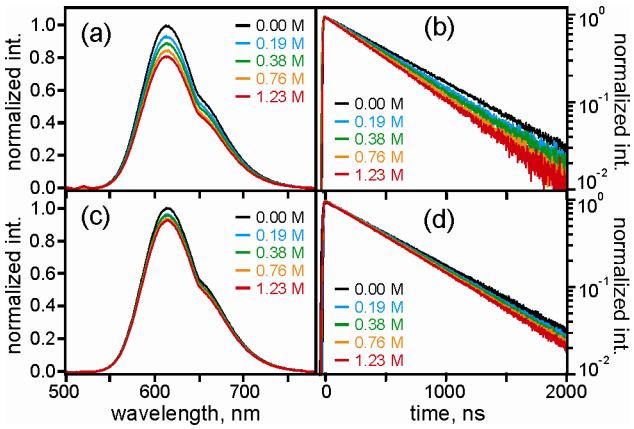

Figure 1. (a) Steady-state luminescence spectra obtained from aerated CH_3CN solutions containing $Ru((CF_3)_2bpy)_3^{2+}$ ($2 \cdot 10^{-5}$ M) in presence of a fixed concentration of CH_3-PhOH (42 mM) but variable pyridine concentrations (see inset); (b) luminescence decays detected at 610 nm after excitation of the same solutions at 532 nm with laser pulses of ~10 ns duration. (c) Analogous experiments as in Figure 1a but with CH_3-PhOD; (d) analogous plot as in Figure 1b but for CH_3-PhOD.

Phenols form hydrogen bonds to pyridine in aprotic solution.[5a, 5j, 14] Hydrogen-bonded phenols in turn are known to have markedly less positive oxidation potentials than non-hydrogen-bonded phenols because electron release is coupled to deprotonation. In other words, phenol oxidation in presence of proton acceptors is a PCET process.[2a, 5b, 15] It has been demonstrated that the

lowering of the oxidation potentials is so substantial that this effect can only be satisfactorily explained in terms of a CPET mechanism.[15] The $Ru((CF_3)_2bpy)_3^{2+}$ luminescence quenching mentioned above for the 6 phenol / pyridine systems is the consequence of the lowering of the phenol oxidation potentials in presence of the proton acceptor pyridine. In fact, our experimental observations are conceptually analogous to those first made by Linschitz with triplet-excited C_{60} and hydrogen-bonded phenols.[5a, 14]

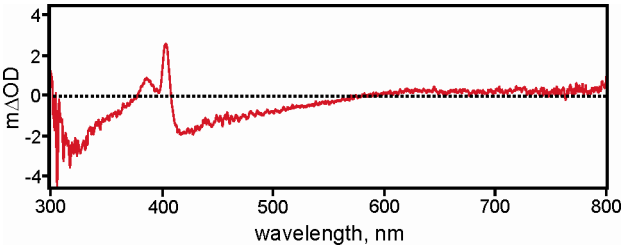

Figure 2. Transient difference spectrum obtained after excitation of an aerated CH_3CN solution containing $7 \cdot 10^{-5}$ M $Ru((CF_3)_2bpy)_3^{2+}$, 0.3 mM CH_3-PhOH, and 1.0 M pyridine at 532 nm with laser pulses of ~10 ns duration. Detection occurred by time-integration over an interval of 5 μs starting 2 μs after excitation.

Direct evidence for PCET photoproducts comes from transient absorption spectroscopy measured after selective $Ru((CF_3)_2bpy)_3^{2+}$ excitation at 532 nm with laser pulses of ~10 ns duration. An exemplary set of data, obtained from an aerated CH_3CN solution containing $7 \cdot 10^{-5}$ M $Ru((CF_3)_2bpy)_3^{2+}$, 0.3 M CH_3-PhOH, and 1.0 M pyridine is shown in Figure 2. The absorption spectrum of 4-methylphenoxyl radical (Me-PhO·) is observed with characteristic peaks at 404 and 386 nm;[16] the bleach around 430 nm is caused by disappearance of $Ru((CF_3)_2bpy)_3^{2+}$ ^{1}MLCT absorption. Analogous transient absorption spectra were obtained for the 5 other phenol /

pyridine combinations, in each case providing unambiguous evidence for the formation of charge-neutral phenoxyl radicals (Figure S9).[16-17] The latter are clearly the products of a photoinduced PCET reaction.

Hydrogen-bonding equilibrium between phenols and pyridine. In CH_3CN solution, there is chemical equilibrium between free phenol (R-PhOH) and pyridine (py) on the one hand and hydrogen-bonded phenol-pyridine adducts (R-PhOH···py) on the other hand (eq. 1).

$$\text{R-PhOH} + \text{py} \leftrightarrows \text{R-PhOH}\cdots\text{py} \qquad \text{(eq. 1)}$$

Any quantitative analysis of the emission quenching data must take this equilibrium into account because only the hydrogen-bonded R-PhOH···py adducts induce significant photoreaction for most phenols (see above). In a given solvent (CH_3CN) at a given temperature (22 °C), the equilibrium (or association) constant (K_A) is primarily a function of the phenol R-substituent.

One possibility to determine the equilibrium constant for the formation of hydrogen-bonded phenol-pyridine adducts is to make use of steady-state luminescence quenching data.[5d, 5g] However, this procedure leads to inconsistencies in the cases considered here. A method based on UV-Vis absorption changes upon addition of large quantities of pyridine to dilute solutions of phenols as reported earlier turned out to be impractical in our cases, mainly due to mutual overlap of the absorption bands of phenol and pyridine.[5a] Consequently, the association constants between the various phenols and pyridine-d_5 were determined by ^{1}H NMR spectroscopy in CD_3CN.

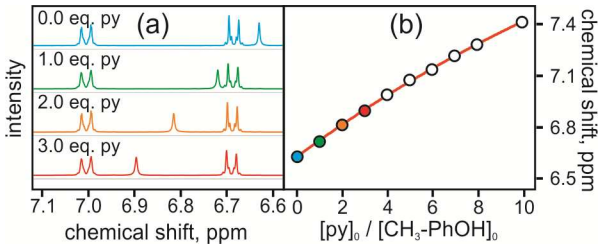

Figure 3. (a) Top: Extract of the ^{1}H NMR spectrum of a 25 mM solution of CH_3-PhOH in CD_3CN at 22 °C. Spectra of the same solution with 1, 2, and 3 equivalents of pyridine-d_5 present are shown below. (b) Chemical shift of the O-H resonance as a function of pyridine-d_5 concentration in ppm; data extracted from Figure 3a and Figure S11. $[py]_0$ is the nominal pyridine-d_5 concentration, $[CH_3\text{-PhOH}]_0$ is the nominal 4-methylphenol concentration; the latter was kept constant at 25 mM throughout the NMR titration experiment.

In Figure 3a the ^{1}H NMR spectrum of 25 mM CH_3-PhOH in CD_3CN at 22 °C is shown. The resonance of the phenolic proton under these conditions is at 6.64 ppm. With 25 mM (= 1 equivalent) pyridine-d_5 present the O-H resonance shifts to 6.72 ppm, and when increasing the pyridine concentration further, the respective signal is shifted further downfield. The chemical shift of the O-H resonance in CD_3CN at 22 °C as a function of pyridine concentration (while keeping the CH_3-PhOH concentration constant) is shown in Figure 3b. The solid line in Figure 3b is the result of a fit to the NMR titration data in the so-called fast-exchange limit, see Supporting Information for further details.[18] An association constant of 1.1±0.1 M^{-1} is determined for CH_3-PhOH and pyridine-d_5 in CD_3CN at 22 °C (Table 2). Analogous ^{1}H NMR titrations with the 5 other phenols (Figures S10-S15) produced the K_A values reported in Table 2; the error bars correspond to the standard deviations resulting from the fits to the experimental data.

Table 2. Equilibrium constants for formation of hydrogen-bonded phenol-pyridine-d_5 adducts in CD_3CN at 22 °C (K_A, eq. 1) determined from ^1H NMR titration experiments with pyridine-d_5 (Figures S10-S16). Abraham's hydrogen bonding parameters (α_2^H) for phenols.[19]

R	K_A [M^{-1}]	α_2^H
OCH_3	1.2±0.1	0.550
CH_3	1.1±0.1	0.571[a]
H	1.1±0.1	0.596
Cl	1.5±0.1	0.670
Br	1.4±0.1	0.674
CN	2.1±0.1	0.787

[a] Value for 4-(*tert.*-butyl)phenol taken as an approximation for the unknown value of CH_3-PhOH.

The association constants in Table 2 are found to increase with increasing hydrogen bond donor ability of the involved phenol. The hydrogen bond donor ability is captured by Abraham's hydrogen bonding parameters (a_2^H) given in the last column of Table 2.[19]

Determination of CPET rate constants. The steady-state luminescence quenchings such as that shown in Figure 1a are accompanied by a shortening of the luminescence lifetime. The data in Figure 4a was measured using aerated CH_3CN solutions containing $2 \cdot 10^{-5}$ M $Ru((CF_3)_2bpy)_3^{2+}$, 42 mM CH_3-PhOH, and pyridine concentrations ranging from 0 to 1.9 M (see inset), i. e., these are the same solutions as those employed for obtaining the data from Figure 1a. Analogous experiments, making use of 532-nm laser excitation pulses of ~10 ns duration, were performed

for the 5 other phenol / pyridine couples, and the respective data are given in the Supporting Information (Figures S17 – S21). All luminescence decays are single exponential over at least two orders of magnitude, and decay rate constants (k_{obs}) were extracted from mono-exponential fits to the experimental decay data. We recall that addition of up to 1 M pyridine to $2 \cdot 10^{-5}$ M solutions of $Ru((CF_3)_2bpy)_3^{2+}$ in aerated CH_3CN does not lead to any changes in luminescence lifetime (Figure S8b). Figure 4b contains a plot of k_{obs} versus pyridine concentration for the CH_3-PhOH / pyridine system. Analogous plots for the 5 other phenol / pyridine couples can be found in the Supporting Information (Figures S17 – S21).

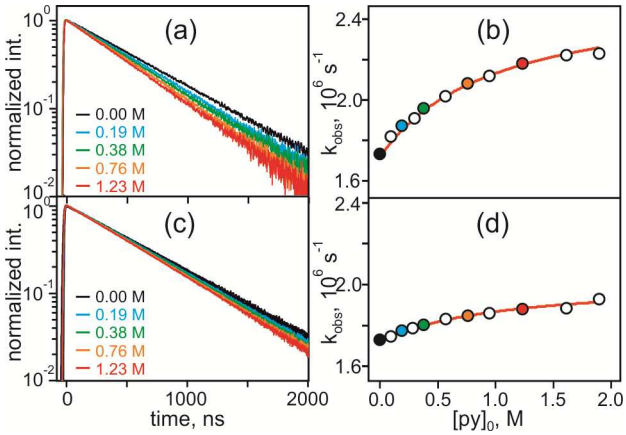

Figure 4. (a) ^{3}MLCT luminescence decays measured after excitation of an aerated CH_3CN solution containing $Ru((CF_3)_2bpy)_3^{2+}$ ($2 \cdot 10^{-5}$ M) in presence of a fixed concentration of CH_3-PhOH (42 mM) and variable pyridine concentrations (see inset); same data as in Figure 1b. Excitation occurred at 532 nm with pulses of ~10 ns duration, detection was at 610 nm; (b) plot of excited-state decay rate constants (k_{obs}, extracted from the ^{3}MLCT luminescence decays in (a) (and from additional decay data not included in (a)) as a function of nominal pyridine concentration; the CH_3-PhOH concentration was 42 mM; (c) Same experiment as in (a) but with

deuterated 4-methylphenol (CH_3-PhOD); same data as in Figure 1d; (d) analogous plot based on the lifetime data from (c) for which deuterated 4-methylphenol (CH_3-PhOD) was used.

For all 6 phenol / pyridine combinations, the observed $Ru((CF_3)_2bpy)_3^{2+}$ luminescence decay rate constants (k_{obs}) are a function of the intrinsic ^{3}MLCT excited-state decay (k_0), the excited-state decay caused by simple (i. e., not proton-coupled) electron transfer to the phenols (k_{ET}), and the contribution to excited-state quenching via CPET involving hydrogen-bonded phenol-pyridine adducts (k_{CPET}) as reflected by the three summands appearing in eq. 2.[5a, 5g, 14]

$$k_{obs} = k_0 + k_{ET}\cdot[\text{R-PhOH}] + k_{CPET}\cdot[\text{R-PhOH}\cdots\text{py}] \quad \text{(eq. 2)}$$

The intrinsic excited-state decay rate constant (k_0) is readily available from a luminescence lifetime measurement of $2\cdot10^{-5}$ M $Ru((CF_3)_2bpy)_3^{2+}$ in pure aerated CH_3CN. This experiment yields $k_0 \approx 1.72\cdot10^6$ s^{-1} (Figure S8b). As noted above, for the phenols with R = CH_3, H, Cl, Br, CN the rate constant k_{ET} is smaller than 10^5 M^{-1} s^{-1}, and the nominal phenol concentrations are 0.3 M or lower. Consequently, the $k_{ET}\cdot$[R-PhOH] term only plays an important role for 4-methoxyphenol for which we have found $k_{ET} = 7\cdot10^7$ M^{-1} s^{-1} (see above). For the 5 other phenols the middle term in eq. 2 can be neglected.

The $k_{CPET}\cdot$[R-PhOH···py] term of eq. 2 accounts for the dependence of k_{obs} on the pyridine concentration. As described in detail in the Supporting Information, k_{obs} can be expressed as a function of the nominal phenol and pyridine concentrations (eq. 3).[5a, 5d, 5g, 14]

$$k_{obs} \approx k_0 + k_{ET} \cdot [R-PhOH]_0 + (k_{CPET} - k_{ET}) \cdot \frac{K_A \cdot [R-PhOH]_0 \cdot [py]_0}{1 + K_A \cdot [py]_0 + K_A \cdot [R-PhOH]_0} \qquad \text{(eq. 3)}$$

Note that eq. 3 is only an approximation because a $[R\text{-}PhOH\cdots py]^2$ summand has been neglected in the denominator of the last term, see Supporting Information for details.

The solid red lines in Figure 4 are the result of fits with eq. 3 to the experimental k_{obs} versus pyridine concentration data using k_{CPET} as the only adjustable parameter. For these fits, k_0 was set to $1.72 \cdot 10^6$ s^{-1}, $k_{ET} = 0$ M^{-1} s^{-1} (the $k_{ET} \cdot [R\text{-}PhOH]_0$ term can be neglected for CH_3-PhOH for reasons explained above), $[R\text{-}PhOH]_0 = 0.042$ M, and $K_A = 1.1$ M^{-1} , i. e., the association constant determined above on the basis of the ^{1}H NMR titration data (second column of Table 2). This procedure yields $k_{CPET} = (1.98 \pm 0.19) \cdot 10^7$ M^{-1} s^{-1} for CH_3-PhOH and $(0.72 \pm 0.16) \cdot 10^7$ M^{-1} s^{-1} for CH_3-PhOD, respectively; the error bars correspond to standard deviations of the fits with eq. 3; the experimental uncertainty associated with the determination of k_{obs} is 5%. Table 3 lists the k_{CPET} values obtained from analogous one-parameter fits to the experimental data for all 6 phenol / pyridine combinations (Figures S17 – S21), using in each case the K_A values from Table 2 as non-adjustable input parameters as well as $k_0 = 1.72 \cdot 10^6$ s^{-1} and $k_{ET} = 0$ M^{-1} s^{-1}, except for CH_3O-PhOH for which $k_{ET} = 7 \cdot 10^7$ M^{-1} s^{-1} was used (see above). The resulting k_{CPET} values range from $(1.25 \pm 0.34) \cdot 10^6$ M^{-1} s^{-1} to $(8.21 \pm 0.21) \cdot 10^8$ M^{-1} s^{-1} (Table 3). This procedure and similar methods for determining k_{CPET} from time-resolved data have been employed earlier.[5a, 5d, 5g, h, 14, 20] Since the ^{1}H NMR titration method from the previous section does not permit determination of association constants between deuterated phenols and pyridine, the K_A values from Table 2 were employed for both ordinary and deuterated phenols.

Table 3. Rate constants for CPET between ^{3}MLCT-excited $Ru((CF_3)_2bpy)_3^{2+}$ and phenol-pyridine adducts (k_{CPET}) in CH_3CN at 20 °C, determined as described in the text.

	R-PhOH	R-PhOD
R	k_{CPET} [M^{-1} s^{-1}]	k_{CPET} [M^{-1} s^{-1}]
OCH_3	$(8.21\pm0.21)\cdot10^8$	$(7.91\pm0.20)\cdot10^8$
CH_3	$(1.98\pm0.19)\cdot10^7$	$(0.72\pm0.16)\cdot10^7$
H	$(4.01\pm0.32)\cdot10^6$	$(2.10\pm0.29)\cdot10^6$
Cl	$(6.32\pm0.43)\cdot10^6$	$(2.40\pm0.36)\cdot10^6$
Br	$(4.99\pm0.41)\cdot10^6$	$(1.25\pm0.34)\cdot10^6$
CN	$(1.54\pm0.06)\cdot10^7$	$(1.20\pm0.06)\cdot10^7$

H/D kinetic isotope effects (KIEs). The occurrence of a significant H/D kinetic isotope effect in the case of 4-methylphenol is evident already from the raw data in Figure 1. For any given pyridine concentration, the luminescence quenching in presence of 42 mM CH_3-PhOD is weaker than in presence of 42 mM CH_3-PhOH, and the luminescence lifetime is shortened less in presence of 42 mM CH_3-PhOD than in presence of 42 mM CH_3-PhOH. Quantitative analysis produces the H/D KIEs summarized in the upper row of Table 4. For comparison, the lower row of Table 4 summarizes the H/D KIEs determined previously for unidirectional CPET between the same 6 phenols and photoexcited $Ru(bpz)_3^{2+}$ (Scheme 1a).

Table 4. H/D kinetic isotope effects for PCET reactions in the systems from Scheme 1.

R	OCH_3	CH_3	H	Cl	Br	CN

bidirectional [a,b]	1.0±0.1	2.8±0.7	1.9±0.3	2.6±0.4	4.0±1.1	1.3±0.1
unidirectional [c,d]	1.0±0.1	1.7±0.2	3.4±0.2	7.8±0.6	2.9±0.2	10.2±0.6

[a] For the systems from Scheme 1b; [b] values correspond to the ratio of k_{CPET} values for ordinary and deuterated reactants from Table 3; [c] for the systems from Scheme 1a; [d] from ref. [7a].

In general KIEs depend on many different parameters and the absence of a sizeable H/D KIE is no argument against CPET, for example because proton and deuteron transfer can proceed through different vibrational states.[21] We recall that the shift of phenol oxidation potentials in presence of hydrogen-bond acceptors can only be satisfactorily explained by invoking CPET.[15] It seems likely that the proton transfer distance has a decisive influence on the magnitude of the KIEs in our systems, as expected by theory and as suspected in other experimental PCET studies.[2b, 22] The proton transfer distance is certainly not identical for the unidirectional PCET reactions in Scheme 1a and the bidirectional PCET reactions in Scheme 1b. An explanation for the large deviation between H/D KIEs observed with 4-cyanophenol in the two types of settings (1.3±0.1 vs. 10.2±0.6) will be given in the next section.

Driving-force dependence of CPET rate constants. For CPET between the reactants from Scheme 1b, the reaction free energy (ΔG_{CPET}^{0}) is basically the difference between the energetic cost associated with homolytic cleavage of the phenolic O-H bonds and the energetic gain associated with reduction of photoexcited $Ru((CF_3)_2bpy)_3^{2+}$ combined with protonation of pyridine. The O-H bond dissociation free energies (BDFEs) for the 6 phenols are known for dimethylsulfoxide solution (fifth column of Table 1).[3, 8] Alternatively, the O-H BDFEs in CH_3CN solution can be estimated on the basis of (gas phase) bond dissociation enthalpies (BDEs) and Abraham's hydrogen bonding parameters as described previously.[8, 13a] Using BDEs

from the literature,[13b] the α_2^H parameters from Table 2,[19a] and $\beta_2^H = 0.44$ for CH_3CN,[8, 13a] one obtains the BDFEs reported in the last column of Table 1 (see Supporting Information for details). These values are remarkably close to the experimental BDFEs determined for DMSO solution, and this finding strongly supports our use of the latter for the following thermodynamic analyses.

Even though the electron and proton acceptors are separate molecules, a *formal* bond dissociation free energy (*f*BDFE) can be calculated for the $Ru((CF_3)_2bpy)_3^{2+}$ / pyridine couple using the standard reduction potential of the oxidant (E_{red}^0) and the pK_a of the conjugate acid of the proton acceptor (eq. 4).[6]

$$f\text{BDFE (X-H) kcal/mol} = 1.37 \cdot pK_a + 23.06 \cdot E_{red}^0 + C_{G,CH3CN} \quad \text{(eq. 4)}$$

The last term in eq. 4 is equivalent to the $H^+/H\cdot$ standard reduction potential in CH_3CN, and it includes the free energy for formation of $H\cdot$ as well as the free energy for solvation of $H\cdot$.[8] For CH_3CN at 298 K, $C_{G,CH3CN} = 54.9$ kcal/mol.[8] The reduction potential of the oxidant (E_{red}^0) is to be used in units of Volts vs. Fc^+/Fc in CH_3CN, and the pK_a value must be for CH_3CN solution.[6] Using $E_{red}^0 = 0.9$ V vs. Fc^+/Fc [9] and $pK_a = 12.5$ [23] one obtains *f*BDFE = 93 kcal/mol. As noted before, the use of formal BDFEs may appear as somewhat peculiar because no X-H bond is formed, but it has been proposed as a useful way to characterize the thermochemistry of a CPET system.[6] Several prior studies confirmed the usefulness of this concept,[8, 24] but the systems from Scheme 1 are special in that the reactants used for unidirectional and bidirectional PCET are as similar as possible.

Thus, the CPET driving-force for the systems in Scheme 1b (ΔG_{CPET}^{0}) is the difference between the experimental O-H BDFEs for the 6 phenols from Table 1 and *f*BDFE = 93 kcal/mol, resulting in ΔG_{CPET}^{0} values ranging from -10 kcal/mol (≈ -0.4 eV) to -0.4 kcal/mol (≈ 0 eV). In our case CPET in CH_3CN produces two monocations ($Ru((CF_3)_2bpy)_3^{+}$ and protonated pyridine) and a neutral species (phenoxyl radicals) out of a dication (photoexcited $Ru((CF_3)_2bpy)_3^{2+}$) and two neutral molecules (phenols, pyridine). The solvation of the individual species may therefore well be significantly different before and after CPET.

Figure 5a shows a semilogarithmic plot of k_{CPET} versus ΔG_{CPET}^{0} for the 6 termolecular ruthenium / phenol / pyridine reaction systems from Scheme 1b. For the phenols with R = OCH_3, CH_3, H, Cl, Br one recognizes a correlation between $\ln(k_{CPET})$ and ΔG_{CPET}^{0} but 4-cyanophenol (yellow data point at ΔG_{CPET}^{0} = -0.4 kcal/mol) stands out. The data in Figure 5a is compatible with CPET as a prevalent PCET reaction mechanism for all phenols except 4-cyanophenol.[4, 7b, 8]

The fact that CN-PhOH stands out is likely an indication for another PCET mechanism. A sequence of rate-determining electron transfer followed by rapid proton transfer (ET-PT) seems highly unlikely based on the relevant redox potentials; initial electron transfer from CN-PhOH to photoexcited $Ru((CF_3)_2bpy)_3^{2+}$ is expected to be endergonic by 0.5 eV (Table 1). The only alternative is then a sequential PT-ET mechanism in which an initial proton transfer step is followed by rapid electron transfer. CN-PhOH is the most acidic of the 6 phenols considered in this work, and based on pK_a values of 22.7 for CN-PhOH and 12.5 for pyridinium in CH_3CN, we estimate that under the experimental conditions used for the luminescence quenching studies up to ~4 μM 4-cyanophenolate (CN-PhO^-) are present. The latter is a strong reductant with E_{ox} = 0.15 V vs. Fc^+/Fc in DMSO and can therefore be expected to quench the ^{3}MLCT excited state of $Ru((CF_3)_2bpy)_3^{2+}$ with a diffusion-limited rate constant. We have attempted fits to the

experimental data with an extended version of eq. 3 containing an additional summand (k_{diff}·[R-PhO$^-$]) reflecting diffusion-limited ($k_{diff} = 1.9 \cdot 10^{10}$ M^{-1} s^{-1} for CH_3CN)[25] reductive excited-state quenching by 4-cyanophenolate; the concentration of the latter was calculated on the basis of $[CN\text{-}PhOH]_0 = 0.15$ M, $[py]_0 = 0 – 2.0$ M, and the abovementioned pK_a values. However, these fits do not provide satisfactory results, possibly because of uncertainties in the acidity constants of 4-cyanophenol and pyridinium in CH_3CN. Yet it seems plausible that the rate constant given for CN-PhOH in Table 3 does not reflect CPET kinetics but rather reflects reaction of a small fraction of 4-cyanophenolate which is formed in a proton transfer pre-equilibrium. The comparatively small H/D KIE of 1.3±0.1 is in line with this interpretation.

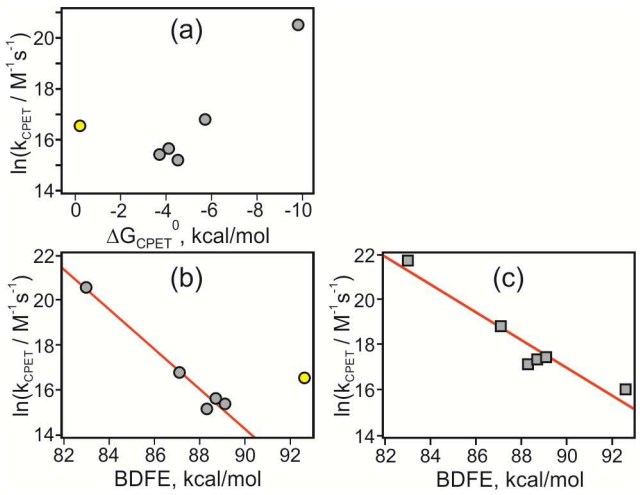

Figure 5. (a) Plot of $\ln(k_{CPET}/M^{-1}\ s^{-1})$ versus ΔG_{CPET}^0 (in kcal/mol) for the termolecular reactions illustrated in Scheme 1b; (b) plot of $\ln(k_{CPET}/M^{-1}\ s^{-1})$ versus O-H BDFEs for the termolecular reactions illustrated in Scheme 1b; (c) plot of $\ln(k_{CPET}/M^{-1}\ s^{-1})$ versus O-H BDFEs for the bimolecular reactions illustrated by Scheme 1a.

Comparison between bi- and unidirectional CPET. Figure 5b plots ln(k_{CPET}) versus O-H BDFEs for the termolecular reactions illustrated in Scheme 1b, and this is merely another representation of the data from Figure 5a. It permits direct comparison with analogous data obtained for the reaction pairs from Scheme 1a in which the same 6 phenols undergo unidirectional CPET with photoexcited $Ru(bpz)_3^{2+}$, a combined electron-proton acceptor requiring no addition of pyridine base.[7] For photoexcited $Ru(bpz)_3^{2+}$ the relevant N-H BDFEs (for hydrogen-atom binding to the N-atoms of the bpz ligand periphery) could not be determined, and therefore in this case k_{CPET} can only be given as a function of phenol O-H BDFEs. The correlations in Figures 5b and 5c (red lines) are typical for hydrogen-atom transfer (HAT) reactions as first discussed by Evans and Polanyi.[4, 26] Thus, bi- and unidirectional CPET with the same set of phenols exhibit a very similar dependence of reaction rates on free energies. The only exception is 4-cyanophenol in the data set of Figure 5b, for reasons discussed above. In the studies of unidirectional (HAT-like) PCET between phenols and photoexcited $Ru(bpz)_3^{2+}$, the 4-cyanophenol data point matches the correlation between ln(k_{CPET}) and O-H BDFE well (Figure 5c).[7] The important difference to the investigations of bidirectional PCET with the termolecular phenol / $Ru((CF_3)_2bpy)_3^{2+}$ / pyridine reaction systems is that in the earlier studies of unidirectional PCET with $Ru(bpz)_3^{2+}$ there is no pyridine which can lead to the formation of a non-negligible amount of 4-cyanophenolate.[7a]

Using the Eyring equation it is possible to estimate activation free energies ($\Delta G_{CPET}^{\ddagger}$) for the CPET processes based on the reaction rate constants (k_{CPET}) from Table 3. Using a prefactor of Z = 10^{11} M^{-1} s^{-1} in the Eyring equation, one obtains $\Delta G_{CPET}^{\ddagger}$ values ranging from 2.8±0.3 kcal/mol for CH_3O-PhOH to 5.9±0.6 kcal/mol for H-PhOH.[27] The respective activation free energies are plotted against the phenol O-H BDFEs in Figure 6a. An analogous plot of $\Delta G_{CPET}^{\ddagger}$ values versus

phenol O-H BDFEs based on data for unidirectional CPET between the reaction pairs from Scheme 1a is shown in Figure 6b.[7a]

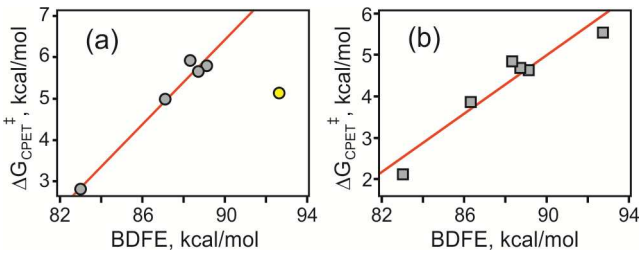

Figure 6. (a) Plot of activation free energies (estimated on the basis of the k_{CPET} values from Table 3 and the Eyring equation with a prefactor of $Z = 10^{11}$ M^{-1} s^{-1}) versus O-H BDFEs for the termolecular reactions systems from Scheme 1b; (b) analogous plot for the bimolecular reactions systems from Scheme 1a.[7a]

$\Delta G_{CPET}^{\ddagger}$ is experimentally more accurately accessible by measurement of the temperature-dependence of the termolecular CPET reactions. Figure 7 contains a plot of $\ln(k_{CPET})$ versus inverse temperature for the reaction with CH_3-PhOH. For the purpose of acquiring the relevant experimental data, sets of time-resolved luminescence data as illustrated in Figure 4 were acquired at 6 different temperatures, and k_{CPET} was determined for each temperature based on the K_A value obtained from ^{1}H NMR titrations at 22 °C. Using the Eyring equation (in combination with the relationship $\Delta G_{CPET}^{\ddagger} = \Delta H_{CPET}^{\ddagger} - T \cdot \Delta S_{CPET}^{\ddagger}$) as a fit function for the experimental data in Figure 7, one extracts $\Delta G_{CPET}^{\ddagger}$ = 5.0±0.6 kcal/mol. The activation enthalpy amounts to $\Delta H_{CPET}^{\ddagger}$ = 2.6±0.4 kcal/mol, the activation entropy is $\Delta S_{CPET}^{\ddagger}$ = -8.1±0.9 cal·K^{-1}·mol^{-1}.

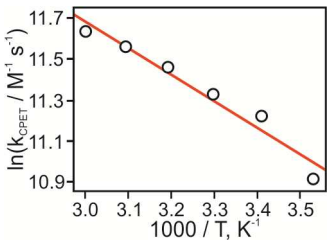

Figure 7. Plot of $\ln(k_{CPET})$ against inverse temperature for the termolecular reaction between photoexcited $Ru((CF_3)_2bpy)_3^{2+}$, CH_3-PhOH, and pyridine in CH_3CN.

In the framework of the adiabatic Marcus equation, barriers and rate constants are governed by only two parameters, namely the reorganization energy (λ_{CPET}) and reaction free energy (ΔG_{CPET}^0). This Marcus treatment predicts that $\Delta\Delta G_{CPET}^{\ddagger}/\Delta\Delta G_{CPET}^0 = 0.5 + \Delta G_{CPET}^0 / 2{\cdot}\lambda_{CPET}$, where $\Delta G_{CPET}^{\ddagger}$ is the activation free energy. Linear regression fits to the data in Figure 6 (excluding the yellow data point for 4-cyanophenol in Figure 6a) yield slopes ($\Delta\Delta G_{CPET}^{\ddagger}/\Delta\Delta G_{CPET}^0$) of 0.52±0.05 for bidirectional and 0.37±0.05 for unidirectional CPET, respectively. The finding that both of these two slopes are close to 0.5 is compatible with CPET reactions that take place with low driving forces, in particular with $-\Delta G_{CPET}^0 << \lambda_{CPET}/2$.[28] Given a maximal free energy of -0.4 eV (see above), it would appear then that $\lambda_{CPET} > 0.8$ eV (18.5 kcal/mol) in our systems. In the adiabatic version of Marcus theory, when ΔG_{CPET}^0 is close to zero, the reorganization energy (λ_{CPET}) is close to double of $\Delta G_{CPET}^{\ddagger}$. The lowest ΔG_{CPET}^0 for the termolecular reactions from Scheme 1b is expected for Br-PhOH (CN-PhOH does not appear to react predominantly via CPET, see above). Based on $k_{CPET} = (4.99\pm0.41){\cdot}10^6$ M^{-1} s^{-1} for Br-PhOH (Table 3), one finds $\Delta G_{CPET}^{\ddagger}$ = 5.9±0.6 kcal/mol and λ_{CPET} = 11.8±1.2 kcal/mol. Prior studies of bidirectional CPET with hydrogen-bonded phenols reported reorganization energies > 22 kcal/mol.[15, 29]

SUMMARY AND CONCLUSIONS

Bidirectional and unidirectional CPET involving two chemically very closely related sets of reactants (Scheme 1) exhibit very similar driving-force dependences of reaction rates. This strongly supports the concept of thermodynamic equivalence between separated electron / proton acceptors ($Ru((CF_3)_2bpy)_3^{2+}$, pyridine) and single-reagent hydrogen atom acceptors ($Ru(bpz)_3^{2+}$).[6] Several prior studies have confirmed the usefulness of this concept,[8, 24] but the systems from Scheme 1 are special in that the reactants used for unidirectional and bidirectional PCET are as similar as possible. This permits a direct comparison of the two different reaction types.

In principle one might expect bi- and unidirectional CPET to be associated with substantially different reorganization energies, but in the driving-force range considered here such effects do not clearly manifest.

EXPERIMENTAL SECTION

$Ru((CF_3)_2bpy)_3^{2+}$ was synthesized following a previously reported method.[9] The phenols are commercially available. ^1H NMR spectra were measured in CD_3CN at 22 °C using a Bruker Avance 400 MHz spectrometer. For deuteration, the phenols were stirred in CD_3OD (99.8% isotope purity) under N_2 at 25 °C for 1 hour. Then the solvent was evaporated and the whole procedure was repeated once more. For the measurements of the deuterated phenols, acetonitrile and pyridine were pre-dried over 3 Å molecular sieves, and then distilled after heating to reflux

for 15 minutes over CaH_2. Dry pyridine and CH_3CN were stored over 3 Å molecular sieves under nitrogen atmosphere. Steady-state luminescence spectroscopy occurred on a Fluorolog 3 instrument from Horiba Jobin-Yvon, the excitation wavelength was 450 nm. Time-resolved luminescence and transient absorption studies were conducted on a LP920KS instrument from Edinburgh Instruments using the frequency-doubled output (532 nm) of a Quantel Brilliant b Nd^{3+}:YAG laser for excitation. The pulse duration was ~10 ns. Luminescence decays were detected at 610 nm. The $Ru((CF_3)_2bpy)_3^{2+}$ concentration in the luminescence experiments was $2 \cdot 10^{-5}$ M, the phenol and pyridine concentrations were as indicated in the individual figure captions. The transient absorption measurements occurred by time-integration over a period of 5 μs starting 2 μs after excitation. The $Ru((CF_3)_2bpy)_3^{2+}$ concentration in the transient absorption experiments was $7 \cdot 10^{-5}$ M, the phenol and pyridine concentrations were 0.1 - 0.5 M and 1.0 M, respectively.

ASSOCIATED CONTENT

Additional optical spectroscopic data, ^1H NMR titration data, derivation of equation 3, estimation of BDFEs for CH_3CN solution, error calculation. This material is available free of charge via the Internet at http://pubs.acs.org.

AUTHOR INFORMATION

Corresponding Author

*oliver.wenger@unibas.ch

Author Contributions

The manuscript was written through contributions of all authors. All authors have given approval to the final version of the manuscript.

ACKNOWLEDGMENT

This work was funded by the Swiss National Science Foundation through grant number 200021_146231/1.

REFERENCES

(1) Weinberg, D. R.; Gagliardi, C. J.; Hull, J. F.; Murphy, C. F.; Kent, C. A.; Westlake, B. C.; Paul, A.; Ess, D. H.; McCafferty, D. G.; Meyer, T. J., *Chem. Rev.* **2012,** *112*, 4016.

(2) (a) Mayer, J. M., *Annu. Rev. Phys. Chem.* **2004,** *55*, 363. (b) Hammes-Schiffer, S.; Stuchebrukhov, A. A., *Chem. Rev.* **2010,** *110*, 6939.

(3) Bordwell, F. G.; Cheng, J. P., *J. Am. Chem. Soc.* **1991,** *113*, 1736.

(4) Matsuo, T.; Mayer, J. M., *Inorg. Chem.* **2005,** *44*, 2150.

(5) (a) Biczok, L.; Gupta, N.; Linschitz, H., *J. Am. Chem. Soc.* **1997,** *119*, 12601. (b) Rhile, I. J.; Mayer, J. M., *J. Am. Chem. Soc.* **2004,** *126*, 12718. (c) Magnuson, A.; Berglund, H.; Korall, P.; Hammarström, L.; Åkermark, B.; Styring, S.; Sun, L. C., *J. Am. Chem. Soc.* **1997,** *119*, 10720. (d) Concepcion, J. J.; Brennaman, M. K.; Deyton, J. R.; Lebedeva, N. V.; Forbes, M. D. E.; Papanikolas, J. M.; Meyer, T. J., *J. Am. Chem. Soc.* **2007,** *129*, 6968. (e) Lachaud, T.;

Quaranta, A.; Pellegrin, Y.; Dorlet, P.; Charlot, M. F.; Un, S.; Leibl, W.; Aukauloo, A., *Angew. Chem. Int. Ed.* **2005,** *44*, 1536. (f) Moore, G. F.; Hambourger, M.; Gervaldo, M.; Poluektov, O. G.; Rajh, T.; Gust, D.; Moore, T. A.; Moore, A. L., *J. Am. Chem. Soc.* **2008,** *130*, 10466. (g) Pizano, A. A.; Yang, J. L.; Nocera, D. G., *Chem. Sci.* **2012,** *3*, 2457. (h) Shukla, D.; Young, R. H.; Farid, S., *J. Phys. Chem. A* **2004,** *108*, 10386. (i) Bonin, J.; Costentin, C.; Robert, M.; Savéant, J. M., *Org. Biomol. Chem.* **2011,** *9*, 4064. (j) Salamone, M.; Amorati, R.; Menichetti, S.; Viglianisi, C.; Bietti, M., *J. Org. Chem.* **2014,** *79*, 6196. (k) Cape, J. L.; Bowman, M. K.; Kramer, D. M., *J. Am. Chem. Soc.* **2005,** *127*, 4208. (l) Sun, L. C.; Burkitt, M.; Tamm, M.; Raymond, M. K.; Abrahamsson, M.; LeGourriérec, D.; Frapart, Y.; Magnuson, A.; Kenéz, P. H.; Brandt, P.; Tran, A.; Hammarström, L.; Styring, S.; Åkermark, B., *J. Am. Chem. Soc.* **1999,** *121*, 6834. (m) Hammarström, L.; Styring, S., *Energy Environ. Sci.* **2011,** *4*, 2379. (n) Johansson, O.; Wolpher, H.; Borgström, M.; Hammarström, L.; Bergquist, J.; Sun, L. C.; Åkermark, B., *Chem. Commun.* **2004**, 194. (o) Costentin, C.; Robert, M.; Savéant, J. M.; Tard, C., *Acc. Chem. Res.* **2014,** *47*, 271. (p) Roth, J. P.; Yoder, J. C.; Won, T. J.; Mayer, J. M., *Science* **2001,** *294*, 2524. (q) Megiatto, J. D.; Mendez-Hernandez, D. D.; Tejeda-Ferrari, M. E.; Teillout, A. L.; Llansola-Portoles, M. J.; Kodis, G.; Poluektov, O. G.; Rajh, T.; Mujica, V.; Groy, T. L.; Gust, D.; Moore, T. A.; Moore, A. L., *Nat. Chem.* **2014,** *6*, 423. (r) Eisenhart, T. T.; Dempsey, J. L., *J. Am. Chem. Soc.* **2014,** *136*, 12221.

(6) Waidmann, C. R.; Miller, A. J. M.; Ng, C. W. A.; Scheuermann, M. L.; Porter, T. R.; Tronic, T. A.; Mayer, J. M., *Energy Environ. Sci.* **2012,** *5*, 7771.

(7) (a) Bronner, C.; Wenger, O. S., *J. Phys. Chem. Lett.* **2012,** *3*, 70. (b) Wenger, O. S., *Acc. Chem. Res.* **2013,** *46*, 1517.

(8) Warren, J. J.; Tronic, T. A.; Mayer, J. M., *Chem. Rev.* **2010,** *110*, 6961.

(9) Furue, M.; Maruyama, K.; Oguni, T.; Naiki, M.; Kamachi, M., *Inorg. Chem.* **1992,** *31*, 3792.

(10) Yamaji, M.; Oshima, J.; Hidaka, M., *Chem. Phys. Lett.* **2009,** *475*, 235.

(11) Kütt, A.; Leito, I.; Kaljurand, I.; Soovali, L.; Vlasov, V. M.; Yagupolskii, L. M.; Koppel, I. A., *J. Org. Chem.* **2006,** *71*, 2829.

(12) Isuzu, K., *Acid-Base Dissociation Constants in Dipolar Aprotic Solvents*. Blackwell Scientific Publications: Oxford, 1990.

(13) (a) Warren, J. J.; Mayer, J. M., *Proc. Natl. Acad. Sci. U. S. A.* **2010,** *107*, 5282. (b) dos Santos, R. M. B.; Simoes, J. A. M., *J. Phys. Chem. Ref. Data* **1998,** *27*, 707.

(14) Biczók, L.; Linschitz, H., *J. Phys. Chem.* **1995,** *99*, 1843.

(15) Rhile, I. J.; Markle, T. F.; Nagao, H.; DiPasquale, A. G.; Lam, O. P.; Lockwood, M. A.; Rotter, K.; Mayer, J. M., *J. Am. Chem. Soc.* **2006,** *128*, 6075.

(16) Das, P. K.; Encinas, M. V.; Steenken, S.; Scaiano, J. C., *J. Am. Chem. Soc.* **1981,** *103*, 4162.

(17) Lind, J.; Shen, X.; Eriksen, T. E.; Merenyi, G., *J. Am. Chem. Soc.* **1990,** *112*, 479.

(18) Macomber, R. S., *J. Chem. Ed.* **1992,** *69*, 375.

(19) (a) Abraham, M. H.; Grellier, P. L.; Prior, D. V.; Duce, P. P.; Morris, J. J.; Taylor, P. J., *J. Chem. Soc., Perkin Trans. 2* **1989**, 699. (b) Snelgrove, D. W.; Lusztyk, J.; Banks, J. T.; Mulder, P.; Ingold, K. U., *J. Am. Chem. Soc.* **2001,** *123*, 469.

(20) Chen, J.; Kuss-Petermann, M.; Wenger, O. S., *Chem.-Eur. J.* **2014,** *20*, 4098.

(21) Markle, T. F.; Rhile, I. J.; Mayer, J. M., *J. Am. Chem. Soc.* **2011,** *133*, 17341.

(22) (a) Migliore, A.; Polizzi, N. F.; Therien, M. J.; Beratan, D. N., *Chem. Rev.* **2014,** *114*, 3381. (b) Zhang, M.-T.; Irebo, T.; Johansson, O.; Hammarström, L., *J. Am. Chem. Soc.* **2011,** *133*, 13224.

(23) Kaljurand, I.; Kütt, A.; Soovali, L.; Rodima, T.; Maemets, V.; Leito, I.; Koppel, I. A., *J. Org. Chem.* **2005,** *70*, 1019.

(24) Tarantino, K. T.; Liu, P.; Knowles, R. R., *J. Am. Chem. Soc.* **2013,** *135*, 10022.

(25) Murov, S. L.; Carmichael, I.; Hug, G. L., *Handbook of photochemistry, 2nd edition*. Marcel Dekker Inc.: New York, 1993.

(26) Evans, M. G.; Polanyi, M., *Trans. Faraday Soc.* **1938,** *34*, 0011.

(27) We also estimated the activation free energy from temperature-dependence studies (see below) and found these estimates to be associated with relative errors of 11%. The errors associated with our activation free energy estimates which are based on k_{CPET} measurements at a single temperature are therefore assumed to be associated with errors on the order of 11% as well.

(28) Mayer, J. M., *Acc. Chem. Res.* **1998,** *31*, 441.

(29) Schrauben, J. N.; Cattaneo, M.; Day, T. C.; Tenderholt, A. L.; Mayer, J. M., *J. Am. Chem. Soc.* **2012,** *134*, 16635.

SYNOPSIS

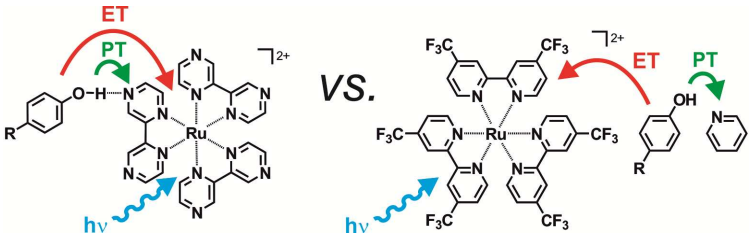

Unidirectional and bidirectional PCET between photoexcited ruthenium complexes and phenolic reaction partners were explored. The two fundamentally different PCET reaction types show roughly the same dependence of reaction rates on phenol *para*-substituents, thereby supporting the concept of thermodynamic equivalence between hydrogen-atom acceptors and separate electron / proton acceptors.